arXiv:astro-ph/9908240v1 21 Aug 1999

Calculating Cross Sections of Composite Interstellar Grains

Nikolai V. Voshchinnikov[1] and John S. Mathis[2]

Received _____; accepted _____

[1] Sobolev Astronomical Institute, Univ. of St. Petersburg; Bibliotechnaya Pl. 2, Stary Peterhof; St. Petersburg, Russia 198904; nvv@aispbu.spb.su

[2]Dept. of Astronomy, Univ. of Wisconsin; 475 N. Charter St., Madison WI 53706, USA; mathis@uwast.astro.wisc.edu

ABSTRACT

Interstellar grains may be composite collections of particles of distinct materials, including voids, agglomerated together. We determine the various optical cross sections of such composite grains, given the optical properties of each constituent, using an approximate model of the composite grain. We assume it consists of many concentric spherical layers of the various materials, each with a specified volume fraction. In such a case the usual Mie theory can be generalized and the extinction, scattering, and other cross sections determined exactly.

We find that the ordering of the materials in the layering makes some difference to the derived cross sections, but averaging over the various permutations of the order of the materials provides rapid convergence as the number of shells (each of which is filled by all of the materials proportionately to their volume fractions) is increased. Three shells, each with one layer of a particular constituent material, give a very satisfactory estimate of the average cross section produced by larger numbers of shells.

We give the formulae for the Rayleigh limit (small size parameter) for multi-layered spheres and use it to propose an "Effective Medium Theory" (EMT), in which an average optical constant is taken to represent the ensemble of materials.

Multi-layered models are used to compare the accuracies of several EMTs already in the literature. EMTs are worse for predicting scattering cross sections than extinction, and considerably worse for predicting g, the mean cosine of the angle of scattering. However, the angular distribution of the scattered radiation depends sensitively on the assumed grain geometry and should be taken with caution for any grain theory. Our computation is vastly simpler than discrete multipole calculations and may be easily applied for practical modeling of the

extinction and scattering properties of interstellar grains.

Subject headings: ISM: Dust, Extinction; Scattering; Methods, Analytical

1. Introduction

Recently there has been considerable progress in the understanding of interstellar dust. Perhaps the most pressing problem is the uncertainty in the reference abundances (the total abundances of elements in the gas *and* dust phases in the interstellar medium; Savage and Sembach 1996; Mathis 1996). A reduction of the reference abundance to about 70% of solar now seems likely. These lower abundances, coupled with the rather large amount of carbon in the gas phase (Sofia, Fitzpatrick, & Meyer 1998), make it very difficult to understand all of the known properties of diffuse interstellar dust while staying within the abundance limits. The abundance constraints can be met better with grains that are composite (Mathis 1996), containing various materials combined with small particles or voids within porous grains, than by nonporous grains as envisioned by models such as "MRN" (Mathis, Rumpl, & Nordsieck 1977) or the very important extension of MRN by Draine & Lee (1984).

A major improvement in our understanding of dust has been brought about by laboratory studies providing refractive indices for most of the likely candidate materials (e.g., Schnaiter et al. 1998, Mennella et al. 1998 for amorphous carbon). These studies must be supplemented by a theory of determining the optical properties of the composite grain, even if the optical constants of each constituent are known. The problem is in determining the influence of the individual components on each other at a microscopic level within the porous grain.

Possible approaches include "Effective Medium Theories," which try to match the polarizability of the composite grain with a hypothetical uniform medium (Bohren & Huffman 1983, hereafter BH; Petrov 1986; Ossenkopf 1991; Lakhtakia & Thompson 1996; Chýlek & Videen 1998; Videen & Chýlek 1998) with an index of refraction that is a suitable superposition of the indices of the constituents. The problem is how to average the indices, and in this paper we compare five recipes with our solution. Other techniques for determining optical properties are the "Discrete Multipole Theories", in which the composite grain is replaced by an array of multipoles (often electric dipoles only, for computational simplicity)

in a specified geometry. The computation determines how each multipole is affected by the incident wave plus all of the other multipoles. This approach is very general and can be used to determine how arbitrarily shaped grains absorb and scatter light as well as such subtleties as the effects of the sizes and shapes of voids within a fluffy grain (e.g., Wolff et al. 1994; Wolff, Clayton, & Gibson 1998). However, it is not practical to model large regions of parameter space (grain size, wavelength, varying amounts of various likely grain constituents) with present computational resources.

Our basic premise is that interstellar grains consist of either very small homogeneous particles/molecules (sizes $\lesssim$ 10 nm) of a particular composition, or else of larger grains with a composite character. The composite grains are formed by agglomeration of the very small grains, and smaller composites, within dense regions. The composites produce most of the interstellar extinction and polarization, and radiate their absorbed energy at mid- and far-infrared wavelengths. They are chemically inhomogeneous, since the individual particles they contain have differing chemical compositions. Many modern grain theories make these assumptions (e.g., Mathis & Whiffen 1989; Désert et al. 1990; Ossenkopf 1993; Weidenschilling & Ruzmaikina 1994, Mathis 1996).

This paper discusses determining *exact* cross sections for the extinction and scattering of an approximate (but probably reasonable) composite grain model. The method outlined here can easily be generalized to include more grain candidates, including a composition gradient within the grain. It provides the cross sections with far less computation than discrete multipole theories.

The assumption is that a composite grain consisting of a random collection of particles of various materials, plus voids, can be replaced by a series of concentric spherical layers, each of which has the optical properties of one material or vacuum. (Hereafter we will consider vacuum to be a material.) Thus, the interactions of the materials within the grain is taken into account. Of course, we make no claim that actual grains consist of concentric layers

(including voids!); the assumption simply mimics the interaction of small particles after they agglomerate into a composite grain while in a dense interstellar environment.

We do not restrict the individual layers of a particular material to be "thin", in the sense that $2\pi\, l/\lambda < 1$, where l is the thickness of the layer, because there is no theory at present to predict the distribution of sizes of the individual particles that go into each composite grain. This size distribution is set by the shattering of grains produced in stellar atmospheres by collisions within the ISM.

In §2 we give a short description of the method of calculation, with the formulae given in Appendix A. Results for various wavelengths, including two types of amorphous carbons, are in §3. There is discussion and a summary in §4.

2. The Calculations

2.1. The General Solution

The theory of interaction of a layered sphere is straightforward in principle, since the eigenfunctions of the scalar wave equation are very well known and the boundary conditions are rather simple (Kerker 1969; BH; Lopatin & Sid'ko 1988; Wu & Wang 1991). We are not aware of the explicit display of the solutions in the astronomical literature and have included an outline of the recursive algorithm we used (Wu & Wang 1991) in Appendix A. These solutions involve the same Riccati-Bessel functions (with the same notation) that occur in the two-layered sphere as given in the subroutine BHCOAT displayed in the appendix of BH.

For illustrative purposes we will consider only composite grains with three materials – silicates, amorphous carbon (AMC), and vacuum. For simplicity, we assumed that the volumes of each of the materials are equal, as is approximately the case for silicates and AMC if the heavy elements are in solar proportions. The 33% vacuum is probably also reasonable.

Each of the three materials is assumed to occur in consecutive concentric spherical layers that form a "shell". The whole grain consists of a specified number, n(shell), of concentric shells, each with the three layers of the materials. In order to determine the effects of geometry, we permuted the order of the material layers within the shells. We found that the order has an effect that converges rapidly with increasing the number of shells (see §3). We varied n(shell) from 1 to 11, but n(shell) = 3 gives an excellent match to the n(shell) = 11 case.

Within each shell the radii of the layers of each material cannot be equally spaced; since the volume fractions are specified, the innermost layer must be relatively thicker than the outer. However, the volumes of the shells can be chosen arbitrarily. If the shells are given equal volumes, the radii of the various zones in the first shell are relatively large: even with 11 shells (33 layers) the innermost layer has $1/33^{1/3} = 31\%$ of the grain radius, while the outermost layer occupies only about 1% of the radius.

With large values of the size parameter of the grain, x ($= 2\pi\, a/\lambda$, with a the radius and λ the wavelength of the radiation outside of the grain), the code has some numerical problems if the materials are very refractive. One set of AMC constants (Schnaiter et al. 1998) produced numerical problems if $kx > 20$ (k is the imaginary part of refractive index). At this large an x, we do not need to be concerned about these problems for astrophysical applications because a substitute is available (see 3.3).

2.2. The Rayleigh Solution and Associated Effective Medium Theory

Farafonov (1999) has produced an expression for the Rayleigh limit ($x \ll 1$, $|m|x \ll 1$, where m is the refractive index) that is useful in some cases. It has advantages over the general solution because it can easily be generalized to any number of similar ellipsoidal layers (i.e., with the same eccentricity). Unlike the results for layered spheres, the polarization of

aligned grains can be computed. Furthermore, there are a great number of astronomical situations, especially at long wavelengths such as the mid-infrared and beyond, where the Rayleigh approximation is an excellent one. Our comparisons show good agreement with the general solution up to $x \sim 1$, or even somewhat larger.

The Farafonov formulae involve the number and materials of the layers as well as the shape of the ellipsoid. We will quote the expressions without derivation.

The interactions of a "small" (Rayleigh) ellipsoid with light can be described completely by the complex electric polarizability, α. The α along each principal axis, $s\,(\equiv x, y, z)$, of the ellipsoid surrounded by vacuum is given by (BH, p. 145):

$$\alpha_s = V\,(\varepsilon - 1)[1 + L_s(\varepsilon - 1)]^{-1}\,, \tag{1}$$

where V is the volume and L_s is the "geometrical factor" associated with the direction s. The values of these factors are given in BH. For spheres, they are 1/3 for each axis.

The extinction cross section, $C_{\rm ext}$, is described by the extinction "efficiency factor", $Q_{\rm ext}$, defined by $C_{\rm ext} = \pi a^2\, Q_{\rm ext}$, and similarly for other cross sections (e.g., scattering). The absorption efficiency of the ellipsoid for radiation with the electric field along the direction s is then $Q_{{\rm abs},s} = 4x\,{\rm Im}\{\alpha_s/V\}$ and the scattering by $Q_{{\rm sca},s} = (8/3)\,x^4|\alpha_s/V|^2$. In the Rayleigh limit, the absorption dominates the scattering because $x \ll 1$, so the absorption is almost equivalent to the extinction.

The α_s for N-layered ellipsoids is (Farafonov 1999)

$$\alpha_s = V\frac{\mathcal{A}_2 - \mathcal{A}_1}{3[(\mathcal{A}_2 - \mathcal{A}_1)L_s + \mathcal{A}_1]}\,; \tag{2}$$

$$\begin{pmatrix} \mathcal{A}_1 \\ \mathcal{A}_2 \end{pmatrix} = \begin{pmatrix} 1 & L_s \\ \tilde{\varepsilon}_N & \tilde{\varepsilon}_N(L_s - 1) \end{pmatrix} \prod_{j=2}^{N-1} \begin{pmatrix} (\tilde{\varepsilon}_j - 1)L_s + 1 & (\tilde{\varepsilon}_j - 1)L_s(L_s - 1)/\tilde{V}_j \\ -(\tilde{\varepsilon}_j - 1)\tilde{V}_j & -(\tilde{\varepsilon}_j - 1)(L_s - 1) + 1 \end{pmatrix} \times$$
$$\times \begin{pmatrix} (\tilde{\varepsilon}_1 - 1)L_s + 1 \\ -(\tilde{\varepsilon}_1 - 1)\tilde{V}_1 \end{pmatrix}\,, \tag{3}$$

where $\tilde{\varepsilon}_i = \varepsilon_i/\varepsilon_{i+1}$ is the relative dielectric constant ($\varepsilon = m^2$) of the layers (j, $j+1$) and $\tilde{V}_j = (a_j\, b_j\, c_j)/(abc)$, the ratio of volume of j-th ellipsoid to the total volume of a particle. The $\tilde{\varepsilon}_N$ for the outermost layer, $j = N$, is the dielectric constant ε_N.

An "Effective Medium Theory" (EMT) is a very commonly used means of estimating the optical properties of composite grains. The whole purpose of an EMT is to predict the dielectric constant that produces the same polarizability as the composite grain. EMTs are fast and simple to use, since they provide the optical constants to be used in an equivalent homogeneous grain. EMTs are, by construction , designed to fit the absorption and scattering properties of the composite grain, since they depend upon the electric polarizability. Other optical effects (especially, the angular pattern of scattering) differ from the extinction in their dependence on the amplitude and phases of the radiation throughout the grain. The use of EMTs is especially dangerous for these properties (see discussion in Chýlek & Videen 1998; Videen & Chýlek 1998).

We can use Equation (2) to define a "Layered-sphere EMT," $\varepsilon_{\rm Lay}$. The relation between the dielectric constant and electric polarization, when $L_s = 1/3$ (i.e., spheres), is

$$\frac{\varepsilon_{\rm Lay} - 1}{\varepsilon_{\rm Lay} + 2} = \frac{\alpha}{V} = \frac{\mathcal{A}_2 - \mathcal{A}_1}{\mathcal{A}_2 + 2\mathcal{A}_1}; \tag{4}$$

$$\varepsilon_{\rm Lay} = (1 + 2\alpha/V)/(1 - \alpha/V) = \mathcal{A}_2/\mathcal{A}_1\,. \tag{5}$$

A program to calculate α is available at the sites that contain the programs for the general layered sphere.

3. Results

We will display the results of various cross sections in a somewhat nonstandard but perhaps useful way. Plots of $Q_{\rm ext}$ against x, where $x \equiv 2\,\pi a/\lambda$, may be less useful than another possibility described below.

An important question is, "What values of x are most relevant at a particular wavelength?" This paper does not try to produce a theory of interstellar grains, but nearly all studies (e.g., Kim, Martin, & Hendry 1994; Kim & Martin 1995) have suggested size distributions something like that of MRN, with a grain size distribution $n(a) \propto a^{-3.5}$. In this case, the extinction optical depth is given by

$$\tau_{\rm ext} = \int n(a)\, C_{\rm ext}\, {\rm d}a \propto \int Q_{\rm ext}\, a^{-1.5} {\rm d}a \;= \int Q_{\rm ext}\, a^{-0.5} {\rm d}\, \ln a\, . \tag{6}$$

For a given wavelength, a is proportional to x. We have, therefore, plotted $Q_{\rm ext}/x^{0.5}$ against x, using a logarithmic axis for x. These plots give directly the integrand of the optical depth integral (the product of the number of particles per unit size times their cross section) if the distribution is like MRN.

The cross sections depend upon x and the optical constants. To illustrate the situations likely to occur in possible grain models, we will present results using optical constants of actual grain candidates: "astronomical silicate" (Draine 1985) and either of two types of AMCs: the "Be 1" tabulated in Rouleau & Martin (1991), or else the "Jena AMC" (Schnaiter et al. 1996)[3]. The "Be 1" reflects the method of preparation of the AMC by Bussoletti et al. (1987) in the laboratory. The two AMC's are very different, reflecting the variations in the method of preparation. We considered the range 1 μm $\geq \lambda \geq$ 0.125 μm, but the behavior of the cross sections is well represented by $\lambda = 0.55$ μm (the V band) and 0.22 μm, for which we present most of our plots and discussion. (The results for the full range of wavelengths will be considered in a future paper on much more detailed grain modeling.) Let us write the index of refraction, m, as $m = n + i\,k$. For (silicate, Be 1 AMC, Jena AMC) at $\lambda = 0.55$ μm we used n = (1.72, 2.08, 2.04); k = (0.030, 0.801, 2.23), respectively. At $\lambda = 0.22$ μm, n =

[3]The indices are available from the site "http://www.astro.uni-jena.de/Group/Subgroups /Labor/Labor/data/carbon/ar.lnk". For a description of the database of optical constants for astronomy see Henning et al. (1999).

(1.87, 1.64, 0.875) and k = (0.02, 0.52, 1.12), respectively. Note the relatively large values of k for the Jena AMC.

3.1. Variations with geometry and number of shells

We first consider whether the order of materials within each shell matters. Figure 1 shows $Q_{\rm ext}/x^{0.5}$ vs. x for vacuum, silicate, and "Be 1" AMC having equal volumes, n(shell) = 3, λ = 0.55 μm, and each shell having the same volume. The six curves represent the permutations of the order of the materials within each shell.

We see that the $Q_{\rm ext}/x^{0.5}$ values vary by $\sim$ 25% in the Rayleigh limit and $\sim$ 15% near the peak extinction. For almost all values of x the extinctions are largest when the vacuum is the innermost material within a shell, since the absorbing materials are then farthest from the center. Usually, the extinction is smallest when the highly absorbing AMC is nearest the center, minimizing its influence, and vacuum farthest, in which case the grain is actually smaller. These trends show why fluffy grains may be more absorbing, per gram, than nonporous ones: the farther the absorbing material from the center, the better it can absorb, per gram.

A behavior similar to that in Figure 1 is shown when each shell has an equal thickness rather than volume. In this case the outer shells, which influence the absorption more than the inner ones, are thicker that when the shell volumes are equal, and the cross sections depend even more strongly upon the order of material than shown in Figure 1.

For larger values of n(shell) permuting the order of materials becomes unimportant. For n(shell) = 11, the spread of the six permutations (not shown) is about half that shown in Figure 1 for three shells, with about the same averaged value at each x. Figure 2 shows $Q_{\rm ext}/x^{0.5}$ vs. x, averaged over the 6 permutations of material order, for n(shell) = 1, 2, and 11. The constants are the same as in Figure 1. We see that there is some deviation at n(shell)

= 1 from larger values of n(shell), but by n(shell) = 2 the cross sections are very close to the values at larger n(shell). The Rayleigh limit (small x) for the averaged n(shell) = 1 is the same as for larger values of n(shell).

For the remainder of this paper, we present results that are averaged among the six permutations of the order of materials within each shell, representing the physical situation of the materials and voids being jumbled together within a composite grain.

3.2. Comparison with Discrete Dipole Calculations

The Discrete Dipole Approximation (DDA) has been used by a number of authors (e.g., Draine & Malhotra 1993; Henning & Stognienko 1993; Wolff, Clayton, & Gibson 1998). These calculations determine the response of an array of dipoles arranged in a cubic lattice with outer boundaries that are as nearly spherical as possible. The strength of each dipole is related to the index of optical constants of the material it simulates.

The results from Wolff et al. (1998) are especially suitable for comparison to multilayered spheres. They considered material similar to silicate at optical wavelengths, with $m = 1.7 + 0.1\,i$, along with voids. They compared two cases: (a) individual dipoles were removed randomly, so the sphere has fine-grained porosity; and (b) each void had 20% of the diameter of the original sphere, with voids falling near the edge of the sphere producing cavities on the surface. Two fractions of vacuum, 40 or 60%, were considered. The size parameters, x, were 1, 4, 7, and 10. In order to average over the effects of the random removals, the calculations are repeated a number of times.

In general, our multilayered spheres gave results intermediate between the DDA with tiny voids (individual dipoles removed) and the large voids (20% of the original sphere's diameter), even in the limit of very large n(shell). An exception is for $x = 1$, when the DDA results were the same for large and small voids, and multilayered spheres gave $Q_{\rm ext}$ 6% larger

for 60% vacuum and 1% smaller for 40% vacuum. For $x = 4$, 40% vacuum, the DDA found $Q_{\rm ext} = (3.20 \pm 0.16)$ for both large and small voids, where the "error" reflects the variations found among various random locations of large voids. Our code gives 3.05 for n(shell) = 50 and 3.15 for n(shell) = 5. For 60% vacuum, the DDA gave $Q_{\rm ext} = 1.92$ (small voids) and 2.15 (large voids); ours gives 2.08. Similar results hold for $x = 7$. For $x = 10$, the DDA for small and large voids gave $Q_{\rm ext} = 2.85$ and 2.5, respectively; ours gives 2.59.

The physical reason why multilayered spheres do not agree with the DDA with small voids is that our geometrical arrangement of the materials is never really random and homogeneous. From the differences of the DDA regarding large and small voids, it is clear that $Q_{\rm ext}$ depends appreciably on the internal geometry of the grain. Our model contains stacked layers throughout, and coherence effects will always be present. On the other hand, there is no reason to believe that the very fine voids modeled in some DDA calculations with very small voids are physically correct. Almost surely real grains are rough surfaced, irregular, and have their materials arranged in pieces that may occupy an appreciable fraction of their size. Thus, there is considerable uncertainty in any detailed model of grains.

Another comparison is with a four-material grain for which a DDA calculation was kindly provided by M. Wolff (private communication, 1996). The materials are silicate, AMC, FeO, and vacuum, with fractions of 0.421, 0.233, 0.046, and 0.3, respectively. The DDA was provided for $x = 0.10$, with the materials placed randomly in an array of 113104 dipoles. For $x = 0.10$, our code gave $Q_{\rm ext} = 0.083$, 79% of the DDA value. The difference persists for large n(shell) and is not caused by the variations among the individual permutations of the materials. Even in the Rayleigh limit, our grain model does not represent arbitrarily fine inclusions. Probably real grains do not either.

3.3. EMTs and Variations with Wavelength

We tested five EMTs: (a) the layered-sphere EMT (§2.2); (b) the "Bruggeman rule" (BH); (c) a modification of it, which averages over grains of different shapes, perhaps simulating the complex structures of layered spheres and real composite grains (Ossenkopf 1991; Stognienko, Henning, & Ossenkopf 1995)[4]; and (d) two versions of the Garnett Rule, often called the "Maxwell Garnett Rule." This rule considers one material as a matrix into which the others are embedded. We used either AMC or silicates as the matrix.

Figure 3*a* shows the accuracy of EMTs at $\lambda = 0.55$ μm. The AMC was Be 1, and n(shell) = 3. The solid line shows $Q_{\rm ext}/x^{0.5}$ for layered spheres, averaged over the permutations of the order of the materials. The other lines are for the five EMTs as indicated in the figure. The matrix for the Garnett EMT is noted.

Figure 3*b* shows that EMTs are not always accurate in the Rayleigh limit, as Figure 3*a* might suggest. It shows the results for a hypothetical material with $(n, k) = (1.4, 2.5)$ in place of the AMC, along with $(n, k) = (1.7, 0.03)$ for the silicate, which are close to the real optical constants. The lines have the same meaning as in Figure 3*a*. By construction, the Layered-sphere EMT is accurate in the Rayleigh limit, but the others are not. The Bruggeman rule did rather well (∼15% too low). In general, the Ossenkopf rule does very well for $x \lesssim 1$ (9% too low in this case) and is almost always superior to the Bruggeman rule. Unfortunately, most of the extinction integral occurs for $x > 1$ for near-infrared and shorter wavelengths, where the EMTs are not very accurate for the constants in Figure 3*a*.

Figure 3 shows that EMTs provide rather accurate extinction cross sections at large x, where the layered-sphere code has some numerical difficulties for very refractive materials. The EMTs use homogeneous sphere calculations that are very stable and can be extended to

[4]With only spherical grains, this Ossenkopf formulation provides the standard Bruggeman rule.

large values of kx, where our multi-layer code encounters difficulties.

EMTs are often rather inaccurate near the maximum extinction. For some sets of optical constants, one or more EMTs can be accurate near the peak, but we find no simple relation that predicts which EMT is the best, or how reliable it is.

Other wavelengths show results qualitatively similar to those in Figure 3, except that the peak shifts because of the changes in optical constants. For $\lambda = 0.22$ μm, the peak occurs near $x = 2.8$; for $\lambda = 0.125$ μm, it is at $x = 1.9$. The EMTs predict the peak position rather well but suggest too large an extinction near the peak (see Figure 3a), meaning that they give the correct values of the real part of refractive index n and values of the imaginary part k that are too small.

Our recommendation is to *use layered-sphere models for composite grains, averaged over the permutations of the ordering of the materials within each shell, with* n*(shell)* $\approx$ *3, in place of any EMT.* If there is an assumed radial gradient of composition, a larger n(shell) is necessary, with the shells varying in composition, but there is no problem in computing the cross sections in such a case.

The cross sections of the composite grains depend strongly upon the optical constants used for the AMC. Figure 4 shows $Q_{\rm ext}/x^{0.5}$ vs. x for both Jena and Be 1 AMC constants, each with 33% silicates and vacuum, for 1.0 and 0.22 μm. The curves are labeled in the figure. We see that there is an appreciable difference in the $\tau_{\rm ext}$ integral between Be 1 and Jena AMC. The Jena AMC curves stop at about $x = 6$ because of instabilities in the code at larger x. At 0.22 μm the difference of the materials is very large, and the Jena AMC will require appreciably less carbon than Be 1.

Figure 4 seems to show that $Q_{ext}(1\,\mu{\rm m})$ (solid curve for Be 1 AMC), integrated over the curves shown in the figure, is larger than the integral of the dot-dashed curve (0.22 μm). It is well known that the opposite is true: the extinction at 0.22 μm is larger than at 1 μm, even

keeping in mind that we are not considering the additional small particles that produce the 2175 Å absorption feature. The paradox arises because the upper limits of the integration are very different; they correspond to approximately the same value of the grain size, a, and not x. The largest grain in MRN is 0.25 μm in radius, at which size the distribution is abruptly truncated. If we assume, for illustration, that the volumes of the largest composite grains are 70% of the sum of the volumes of the largest graphite and silicate grains in MRN, along with 33% vacuum, the radius of the largest composite grain is $0.25\,[2(0.7)/(1-f_{\rm vac})]^{1/3}$ μm, or 0.32 μm. The values of x for this size are 2.0 at 1 μm and 9.25 at 0.22 μm. Figure 4 shows that the upper limit of x at 1 μm will reduce the value of the integral of $Q_{\rm ext}/x^{0.5}$ over the sizes by over a factor of two. The inclusion of the gas-phase carbon, as well as the carbon and silicon in the small grains or molecules producing the red and infrared emission features, will reduce the upper bound on x from that estimated above, which will further reduce the 1 μm extinction relative to the 0.22 μm.

The actual size distribution in a model must be determined from a careful consideration of all of the various demands for materials in the light of all available observational constraints. For instance, the integral over the composite grains does not include any of the small carbon particles that provide additional absorption at 0.22 μm, nor the carbonaceous molecules that produce the infrared emission bands in the 3.28 – 12 μm region.

3.4. Other Grain Properties

Extinction is determined from observations far more accurately than any other grain diagnostic property, but there are estimates (mainly from reflection nebulae) of the albedo and of the phase parameter, g ($\equiv \langle\cos(\Theta)\rangle$, where Θ is the angle of scattering.) Gordon, Calzetti, & Witt (1997) have given reasonable estimates of these parameters as functions of wavelength. Any theory using composite grains should make predictions for them as well as the extinction per H atom. The same coefficients that are used in calculating the extinction

cross sections also give the scattering cross section and the phase parameter by standard formulae (e.g., BH). Here we discuss the accuracy of the EMTs for providing the scattering cross sections and phase parameters. We concentrate upon $\lambda = 0.55$ μm because the optical constants there are very similar to those throughout the optical region of the spectrum where most of the observations exist. All of the results we present apply to this region in general.

Figure 5 shows $Q_{\rm sca}/x^{0.5}$ at 0.55 μm plotted against x. As for $Q_{\rm ext}$, this is the integrand of the optical depth to scattering if the size distribution follows an $a^{-3.5}$ distribution. The layered spheres consist of 33% silicates, vacuum, and each of the two AMCs. The solid line is the layered sphere result (averaged, as usual, over all six permutations).

As expected, the scattering is very small until $x \gtrsim 1$, even with the size distribution assumed to be skewed to small grains ($\propto a^{-3.5}$). For the Be 1 AMC, the EMTs overestimate the scattering cross section because the interval of x does not extend much above 3 because of mass considerations; in this range the EMTs are too large, and the Ossenkopf EMT is better than the Bruggeman. The opposite is true for the Jena AMC; the cross sections are somewhat lower than the layered sphere for $x > 1$ and do not have the correct limit at large x, where they are successful as regards extinction. The Garnett rule with AMC as the matrix is the long-dashed line that is far above the layered sphere near the peak scattering, while the Garnett rule with silicate as the matrix is the closest to the exact solution for Be 1 AMC. Unfortunately, it was often the worst in predicting the extinction (see Figure 3). For Be 1 AMC, the layered sphere lies below all EMTs for $x \leq 3$. From Figure 5 we conclude that EMTs are more unreliable for predicting scattering than for extinction, and which EMT is suitable is not clear.

The prediction of grain properties other than the absorption and scattering cross sections (e.g., the angular distribution of the scattering, or g) is especially dangerous because they depend upon the details of the phases of the scattered wave within the grain, and therefore on the details of the geometry. We will discuss g while keeping this danger in mind. Figure

6 shows $g(x)$ for the same parameters and notation as Figure 5, with Be 1 AMC. For $g(x)$ it is not appropriate to take the size distribution into account because g is not an averaged quantity, but the ratio of two averages:

$$g(x) = \frac{\int \cos(\Theta)\, Q_{\rm sca}\, {\rm d}\cos(\Theta)}{\int Q_{\rm sca}\, {\rm d}\cos(\Theta)} \,. \tag{7}$$

All EMTs predict almost the same $g(x)$, so only one line is plotted. The envelope of deviations among the EMTs is typically ~ 0.01, so a superposition of the individual EMT results merely broadens the dashed line slightly.

As expected, the figure shows that small grains scatter isotropically ($g \sim 0$), and that large grains are forward-throwing ($g \geq 0.6$). For the Be 1 AMC, all of the EMTs do a poor job of predicting g. Their prediction is somewhat better for Jena AMC, but the major point is that in general EMTs are quite unreliable. However, the assumption of spherical grains is also much more problematic for predicting g than for the extinction. For instance, spheres have a strong back scattering from constructive interference of waves with exactly equivalent paths at all azimuthal angles. This scattering is not present in elongated or rough grains.

4. Summary

We have shown that layered spheres provide a simple way to calculate the optical properties of spherical composite grains with an arbitrary degree of vacuum and number of constituent materials, provided the voids or individual constituent particles are small in comparison to the composite grain (as is assumed in all EMTs as well). The variations of the cross sections among the permutations of materials for small numbers of layers (see Figure 1 for three shells, or nine layers) show that there are appreciable effects of structure if the layers are thick in comparison to the size of the grain.

We have given an expression (Farafonov 1999) for the polarizability of a layered sphere in the Rayleigh limit. This expression is quite appropriate for wavelengths in the near

infrared and longer. It can be used to determine the optical properties of nonspherical grains, including polarization introduced when they are aligned, because it contains the shape dependence of the cross sections. We used it to propose an "Layered Sphere Effective Medium Theory", in which an average optical constant is taken to represent the ensemble of materials. Our numerical results show that this EMT applies to surprisingly large values of x for predicting extinction and scattering (Figures 3 and 5), but it fails, along with all of the other EMTs, for predicting g (Figure 6).

We have also shown that the various EMTs are quite approximate, with the largest errors occurring for the scattering cross sections and, especially, for the phase parameter, g. It is somewhat ominous that the EMTs tend to overestimate the extinction cross section, since one of the largest problems facing the understanding of interstellar grains is meeting the cosmic abundance requirements, especially if the reference abundance of the ISM is sub-solar.

The results of multilayered spheres do not represent composite grains with extremely fine-grained constituent particles. There is always a coherence in the assumed geometrical arrangement of the constituent materials. Real cometary and interplanetary grains are also composed of particles that can be appreciable in size as compared to the grain, and probably interstellar grains as well.

The code producing the cross sections for layered spheres, in general and also in the Rayleigh limit, is available from two sources: (a) by anonymous ftp from "ftp.astro.wisc.edu" in the directory "outgoing/mathis"; (b) via Internet: "http: //www.astro.spbu.ru/JPDOC/nmie.html" or "http://www.astro.uni-jena.de/Users/database/nmie.html".

We appreciate the suggestions made by the referee, Geoff Clayton. N.V.V. was partly supported by grants of the Volkswagen Foundation, the program "Astronomy" of the government of the Russian Federation and the program "Universities of Russia – Fundamental

Researches" (grant N 2154). Both authors appreciate conversations with Prof. Th. Henning.

Appendix A. Formulae for Multi-Layered Spheres

We follow the formulation by Wu & Wang (1991). The cross section efficiencies ($Q_{\rm ext}$, etc.) are given as series over an index n involving two complex amplitude coefficients, a_n and b_n (see BH or Kerker 1969 for explicit expressions.) We assume there are N layers, with the j-th layer having a radius a_j, a size parameter $x_j = 2\pi a_j/\lambda$, and a refractive index $m_j = n_j + k_j\, i$. The outer radius is $a = a_N$ and size parameter $x = x_N$. The expressions for coefficients a_n, b_n can be written using the logarithmic derivatives of Riccati-Bessel functions $\psi_n(z)$, $\chi_n(z)$, $\zeta_n(z)$ and the ratios of one function to another, where z is complex:

$$\mathcal{D}_n^{(1)}(z) \equiv \frac{\psi_n'(z)}{\psi_n(z)}\,; \quad \mathcal{D}_n^{(2)}(z) \equiv \frac{\chi_n'(z)}{\chi_n(z)}\,; \quad \mathcal{D}_n^{(3)}(z) \equiv \frac{\zeta_n'(z)}{\zeta_n(z)}\,;$$

$$\mathcal{D}_n^{(l)}(z) = -\frac{n}{z} + \left[\frac{n}{z} - \mathcal{D}_{n-1}^{(l)}(z)\right]^{-1}\,, \quad l = 1,2,3\,;$$

$$\mathcal{B}_n(z) \equiv \frac{\psi_n(z)}{\chi_n(z)} = \mathcal{B}_{n-1}(z)\,\frac{n/z + \mathcal{D}_n^{(2)}(z)}{n/z + \mathcal{D}_n^{(1)}(z)}\,;$$

$$\mathcal{C}_n(z) \equiv \frac{\psi_n(z)}{\zeta_n(z)} = \mathcal{C}_{n-1}(z)\,\frac{n/z + \mathcal{D}_n^{(3)}(z)}{n/z + \mathcal{D}_n^{(1)}(z)}\,.$$

The quantities $\mathcal{D}_n^{(1)}$ are calculated by downward recursion in n, starting with $\mathcal{D}_{NMX}^{(1)} = 1/z$ at the largest value of n, NMX. The other functions above are calculated with forward recursion, starting with

$$\mathcal{B}_0(z) = \psi_0(z)/\chi_0(z) = \sin z/\cos z\,;$$

$$\mathcal{C}_0(z) = \psi_0(z)/\zeta_0(z) = \sin z(\sin z + i\cos z)^{-1}\,;$$

$$\mathcal{D}_0^{(3)}(z) = i\,.$$

The $\mathcal{D}_n^{(2)}(z)$ is best found from

$$\mathcal{D}_n^{(2)}(z) = \left[\mathcal{C}_n(z)\mathcal{D}_n^{(1)}(z) - \mathcal{D}_n^{(3)}(z)\right]\left[\mathcal{C}_n(z) - 1\right]^{-1}\,.$$

Additional functions that vary with the interface radii, x_j $(j = 2, ..., N)$, are defined in terms of the above quantities:

$$\mathcal{H}_n^a(m_j x_j) = \frac{\mathcal{B}_n(m_j x_j)\mathcal{D}_n^{(1)}(m_j x_j) - A_n^{(j)}\mathcal{D}_n^{(2)}(m_j x_j)}{\mathcal{B}_n(m_j x_j) - A_n^{(j)}} \,;$$

$$A_n^{(j)} = \mathcal{B}_n(m_j x_{j-1})\, \frac{m_j \mathcal{H}_n^a(m_{j-1}x_{j-1}) - m_{j-1}\mathcal{D}_n^{(1)}(m_j x_{j-1})}{m_j \mathcal{H}_n^a(m_{j-1}x_{j-1}) - m_{j-1}\mathcal{D}_n^{(2)}(m_j x_{j-1})} \,;$$

$$\mathcal{H}_n^b(m_j x_j) = \frac{\mathcal{B}_n(m_j x_j)\mathcal{D}_n^{(1)}(m_j x_j) - B_n^{(j)}\mathcal{D}_n^{(2)}(m_j x_j)}{\mathcal{B}_n(m_j x_j) - B_n^{(j)}} \,;$$

$$B_n^{(j)} = \mathcal{B}_n(m_j x_{j-1})\, \frac{m_{j-1} \mathcal{H}_n^b(m_{j-1}x_{j-1}) - m_j\mathcal{D}_n^{(1)}(m_j x_{j-1})}{m_{j-1} \mathcal{H}_n^b(m_{j-1}x_{j-1}) - m_j\mathcal{D}_n^{(2)}(m_j x_{j-1})} \,.$$

The calculation starts at the innermost interface, $j = 1$, with

$$A_n^{(1)} = B_n^{(1)} = 0 \,; \quad \mathcal{H}_n^a(m_1 x_1) = \mathcal{H}_n^b(m_1 x_1) = \mathcal{D}_n^{(1)}(m_1 x_1) \,.$$

At the outer boundary of the sphere the desired coefficients a_n and b_n are

$$a_n = \mathcal{C}_n(x)\, \frac{\mathcal{H}_n^a(m_N x) - m_N \mathcal{D}_n^{(1)}(x)}{\mathcal{H}_n^a(m_N x) - m_N \mathcal{D}_n^{(3)}(x)} \,; \quad b_n = \mathcal{C}_n(x)\, \frac{m_N \mathcal{H}_n^b(m_N x) - \mathcal{D}_n^{(1)}(x)}{m_N \mathcal{H}_n^b(m_N x) - \mathcal{D}_n^{(3)}(x)} \,.$$

The efficiency factors follow from these by a series

$$Q_{\rm ext} = \frac{2}{x^2}\sum_{n=1}^{\infty}(2n+1){\rm Re}(a_n + b_n) \,; \quad Q_{\rm sca} = \frac{2}{x^2}\sum_{n=1}^{\infty}(2n+1)(|a_n|^2 + |b_n|^2) \,.$$

REFERENCES

Bohren, C. F., and Huffman, D. R. 1983, Absorption and Scattering of Light by Small Particles, John Wiley and Sons (New York) (BH)

Bussoletti, E., Colangeli, L., Borghesi, A., and Orofino, V. 1987, A&AS, 70, 257

Chýlek, P. & Videen, G. 1998, Optics Comm., 146, 15

Désert, F. X., Boulanger, F., & Puget, J. L. 1990, A&A, 237, 215

Draine, B. T. 1985, ApJS, 57, 587

Draine, B. T., & Lee, H. M. 1984, ApJ, 285, 89

Draine, B. T., & Malhotra, S. 1993, ApJ, 414, 632

Farafonov, V. G. 1999, Optics & Spectroscopy, submitted

Gordon, K. D., Calzetti, D. A., & Witt, A. N. 1997, ApJ, 487, 625

Henning, Th., & Stognienko, R. 1993, A&A, 280, 609

Henning, Th., Il'in, V. B., Krivova, N. A., Michel, B., & Voshchinnikov, N.V. 1999, A&AS, 136, 405

Kerker, M. 1969, *The Scattering of Light and Other Electromagnetic Radiation* (New York: Academic Press)

Kim, S-H., & Martin, P. G. 1995, ApJ, 444, 293

Kim, S-H., Martin, P. G., & Hendry, P. D. 1994, ApJ, 422, 164

Lakhtakia, A. & Thompson, B. J. (eds.) 1996, *Selected Papers on Linear Optical Composite Materials* (SPIE Opt. Ing. Press, Bellingham)

Lopatin, V. N., & Sid'ko, F. Ya. 1988, *Introduction to Optics of Cell's Suspension* (Nauka, Novosibirsk) (in Russian)

Mathis, J. S. 1996, ApJ, 472, 463

Mathis, J. S., Rumpl. W., & Nordsieck, K.H. 1977, ApJ, 217, 425 (MRN)

Mathis, J. S., & Whiffen, G. 1989, ApJ, 341, 808

Mennella, V., Colangeli, L., Bussoletti, E., Palumbo, P., & Rotundi, A. 1998, ApJ, 507, L177

Ossenkopf, V. 1991, A&A, 251, 210

Ossenkopf, V. 1993, A&A, 280, 617

Petrov, Yu. A. 1986, *Clusters and Small Particles*, (Nauka, Moscow) (in Russian)

Rouleau, F. & Martin, P. G. 1991, ApJ, 377, 526

Savage, B. D., & Sembach, K. R. 1996, ARAA, 34, 279

Schnaiter, M., Mutschke, H., Henning, Th., Lindackers, D., Strecker, M., & Roth, P. 1996, ApJ, 464, L187

Schnaiter, M., Mutschke, H., Dorschner, J., Henning, Th., & Salama, F. 1998, ApJ, 498, 486

Sofia, U. J., Fitzpatrick, E. L., & Meyer, D. M. 1998, ApJ, 504, L47

Stognienko, R., Henning, Th., & Ossenkopf, V. 1995, A&A, 296, 797

Videen, G. & Chýlek, P. 1998, Optics Comm., 158, 1

Weidenschilling, S. J., & Ruzmaikina, T. V. 1994, ApJ, 430, 713

Wolff, M. J., Clayton, G. C., Martin, P. G., & Schulte-Ladbeck, R. E. 1994, ApJ, 423, 412

Wolff, M. J., Clayton, G. C., & Gibson, S. J. 1998, ApJ, 503, 815

Wu, Z. P., & Wang, Y. P. 1991, Radio Science, 26, 1393

This manuscript was prepared with the AAS LaTeX macros v4.0.

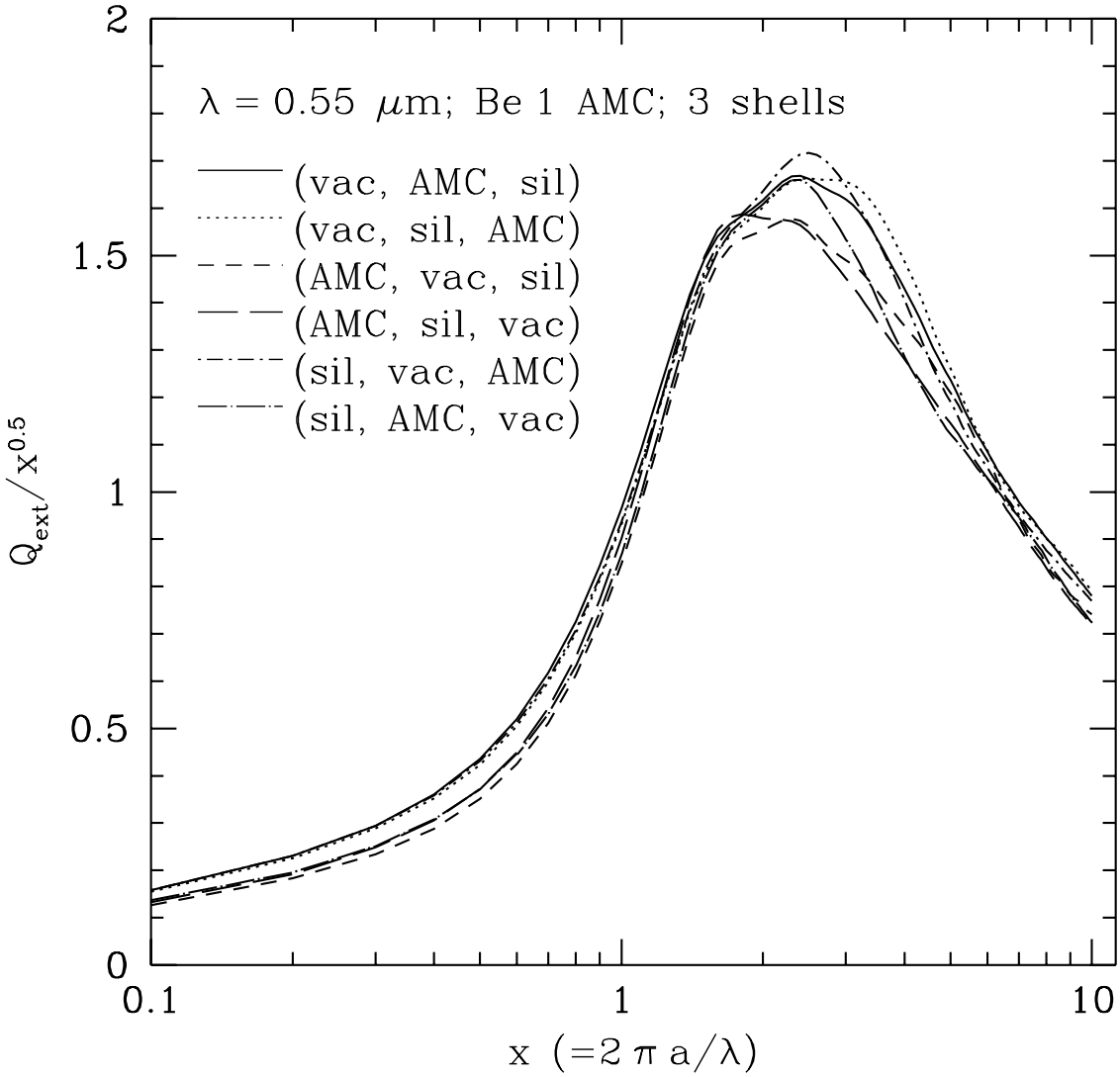

Fig. 1.— The quantity $Q_{\rm ext}/x^{0.5}$, where $Q_{\rm ext}$ is the extinction efficiency of a grain and $x = 2\pi a/\lambda$, plotted against x for the case of 3 shells, each containing equal amounts of vacuum, Be 1 amorphous carbon (Rouleau & Martin 1991), and silicate. The constants are appropriate for $\lambda = 0.55$ μm. The curves give the results for each of the six permutations, as labeled. The quantity plotted is proportional to the integrand of the extinction integral for a size distribution proportional to $a^{-3.5}$, so the maximum of the curves show the value of x at which the contribution of grains is maximal.

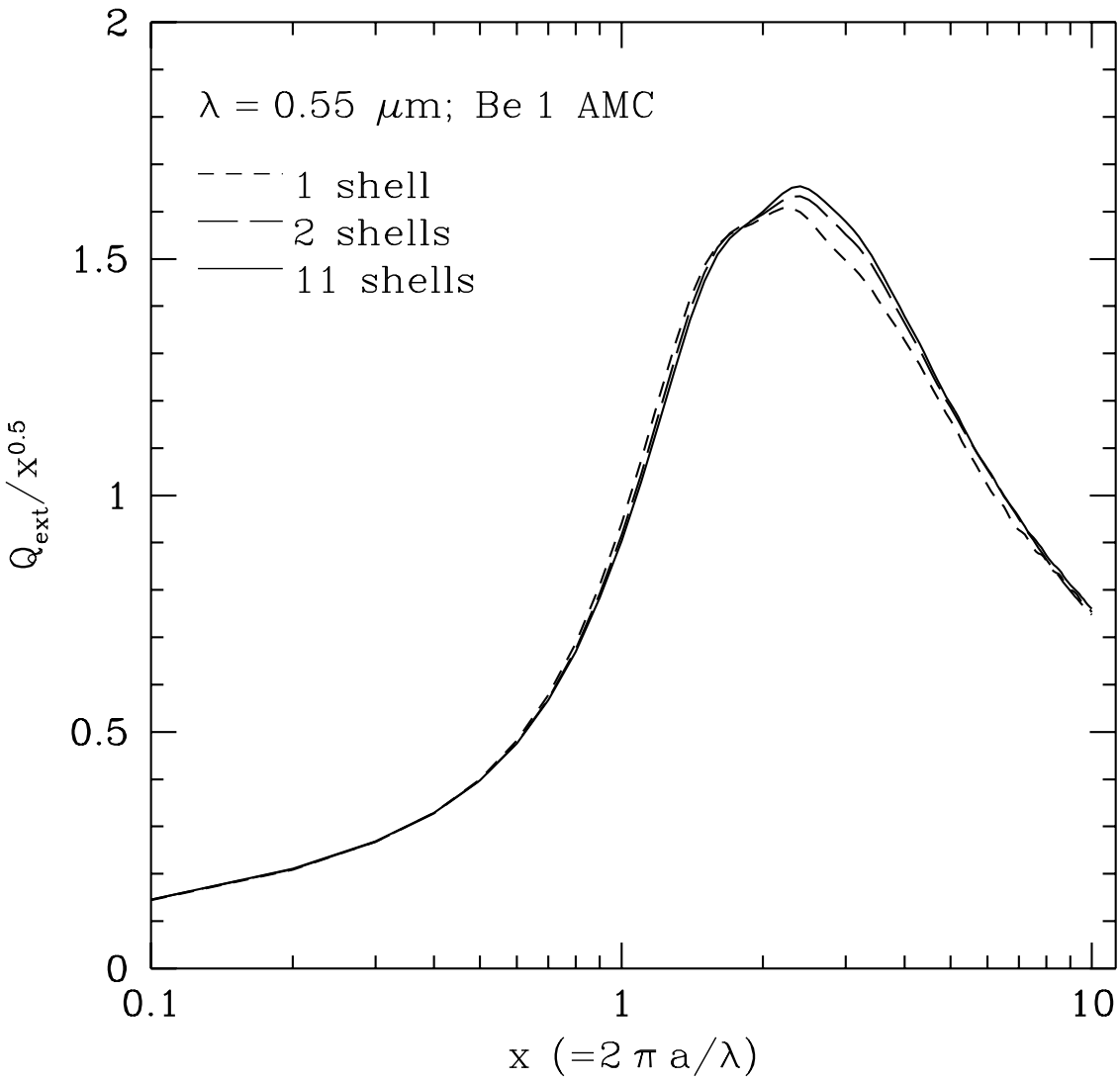

Fig. 2.— The quantity $Q_{\rm ext}/x^{0.5}$plotted against x with the cross sections averaged over all six permutations of the order of materials within each shell (see Figure 1) for three values of n(shell). The optical constants are the same as for Figure 1. The dashed line, dotted line, and solid line are for n(shell) = 1, 2, and 11, respectively. The lines for n(shell) ≥ 5 are coincident with the solid line.

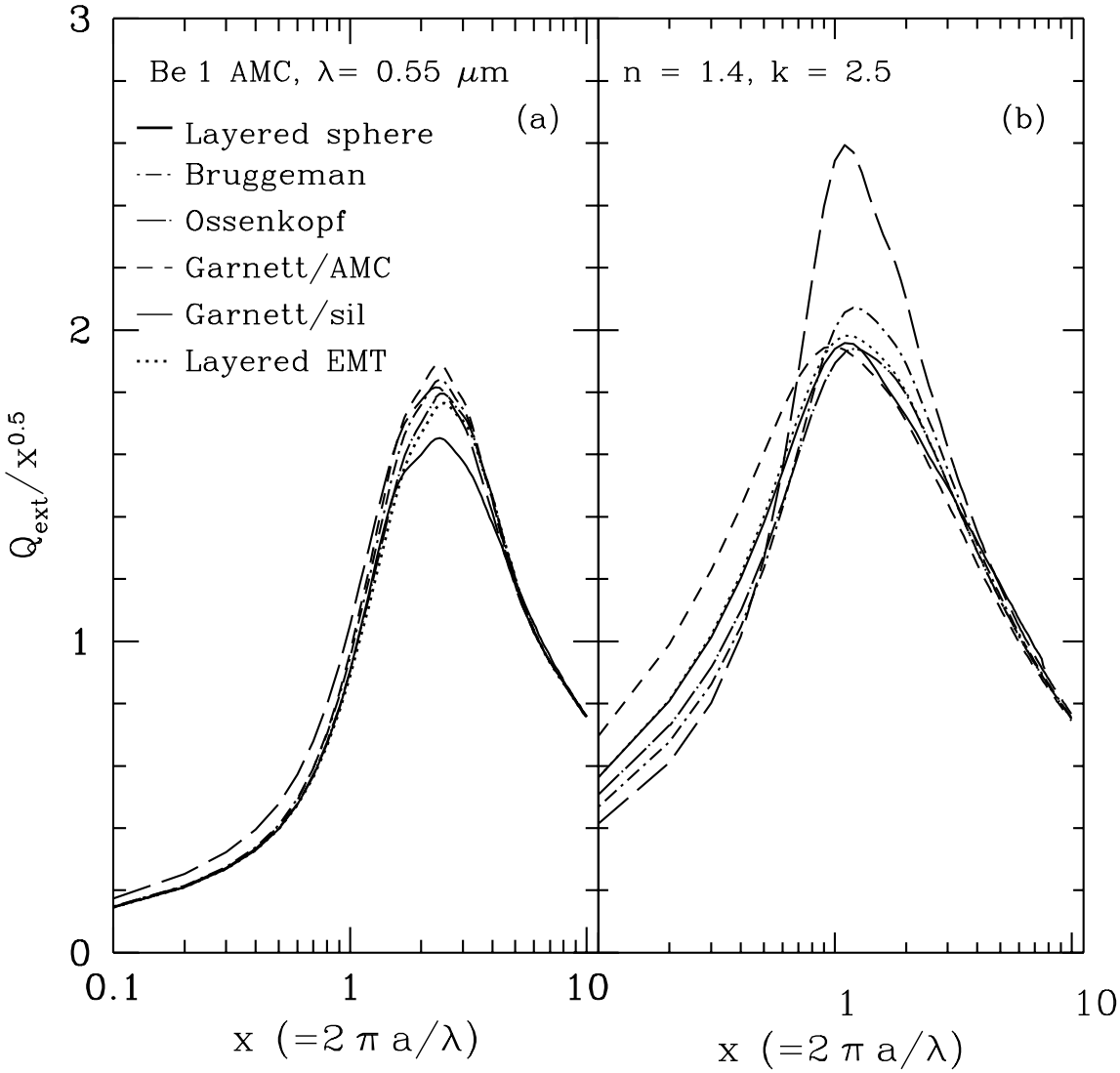

Fig. 3.— $Q_{\rm ext}/x^{0.5}$ plotted against x with the cross sections from various Effective Medium Theories (labeled) and also for the averaged over all six permutations of the order of materials within each shell (see Figure 1). Vacuum, AMC, and silicate each comprise 33% of the volume. The Garnett rule assumes one material, as distinguished in the label, is the matrix in which the others are embedded. The "Layered EMT" is described in this paper. The AMC constants are (a), Be 1; (b) a hypothetical material with (n, k) = (1.4, 2.5). We see that the EMTs uniformly overestimate the cross section near the peak in (a) and are rather inaccurate at small x in (b).

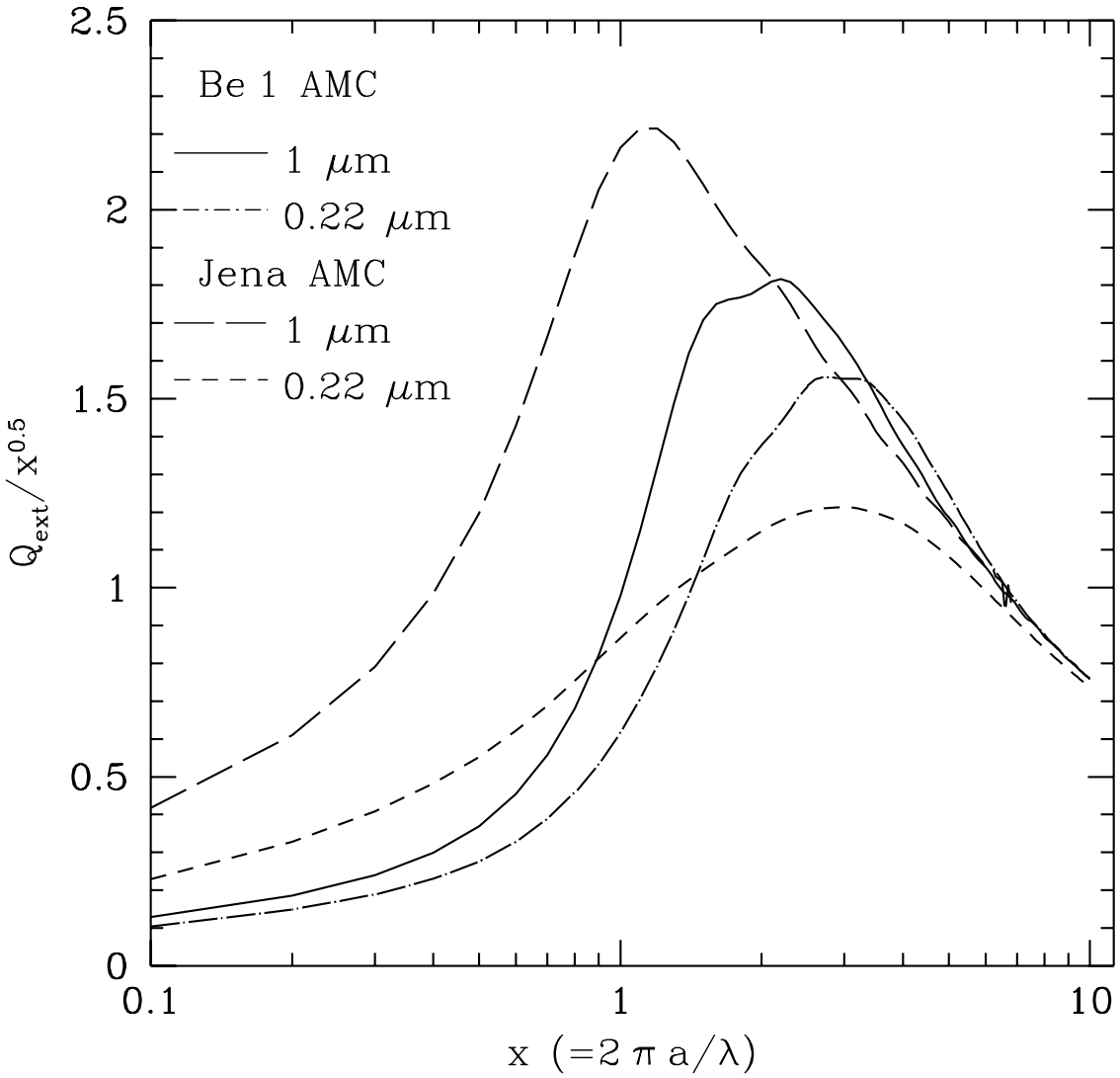

Fig. 4.— $Q_{\rm ext}/x^{0.5}$ vs. x for two AMCs, two wavelengths, as labeled. Note the very large difference in the cross sections for the two types of AMC at the same wavelength.

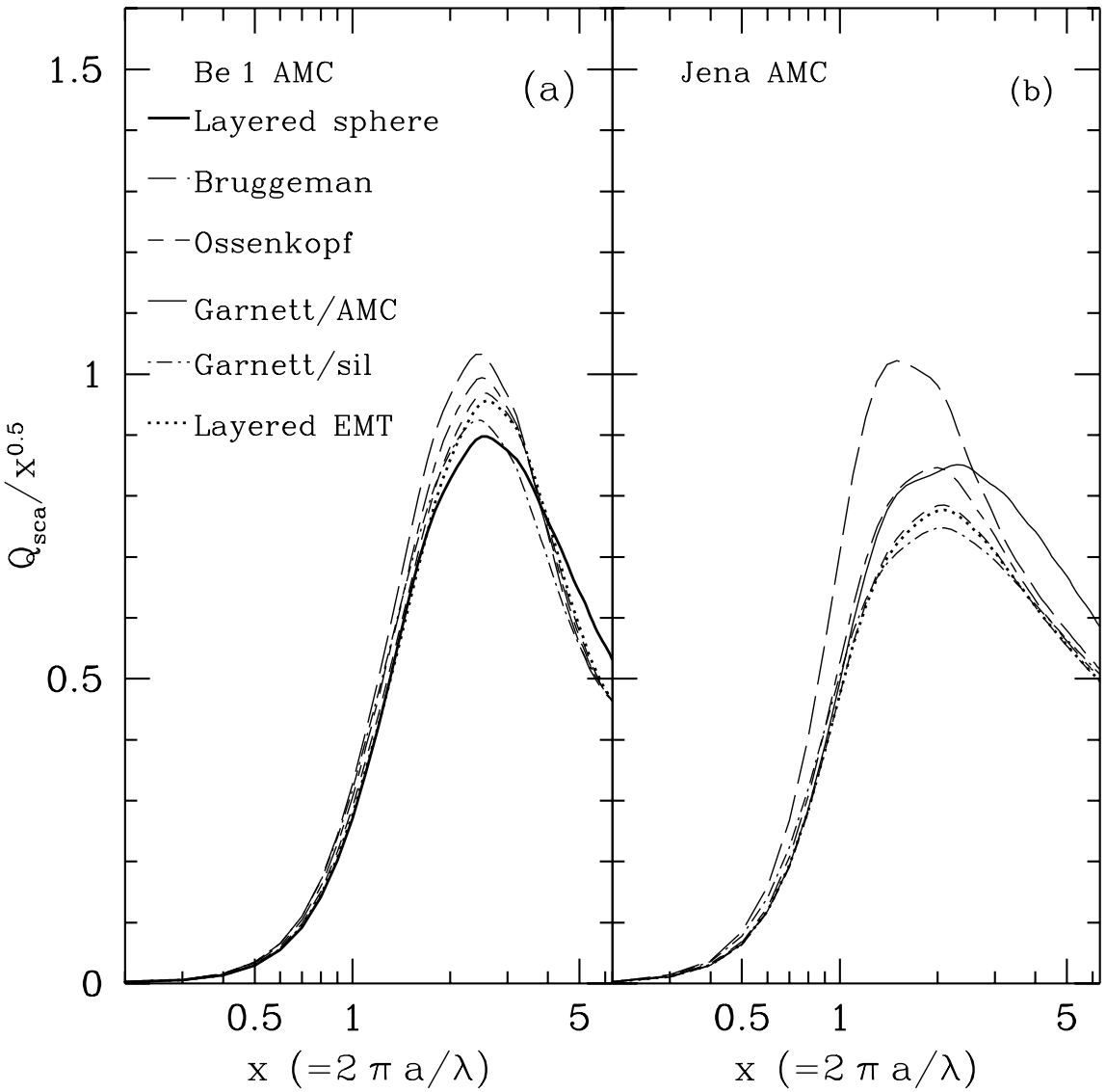

Fig. 5.— $Q_{\rm sca}/x^{0.5}$ vs. x, whose integral over $\log(x)$ gives the optical depth for scattering, for layered spheres (33% each of vacuum, silicate, and amorphous carbon). The predictions of various Effective Medium Theories, as indicated in the label, are also shown. The wavelength is 0.55 μm. In Figure (a) the AMC is Be 1; in (b), Jena. The Garnett EMT with silicate as the matrix represents the scattering rather well, but it is worst for the extinction (see Figure 3).

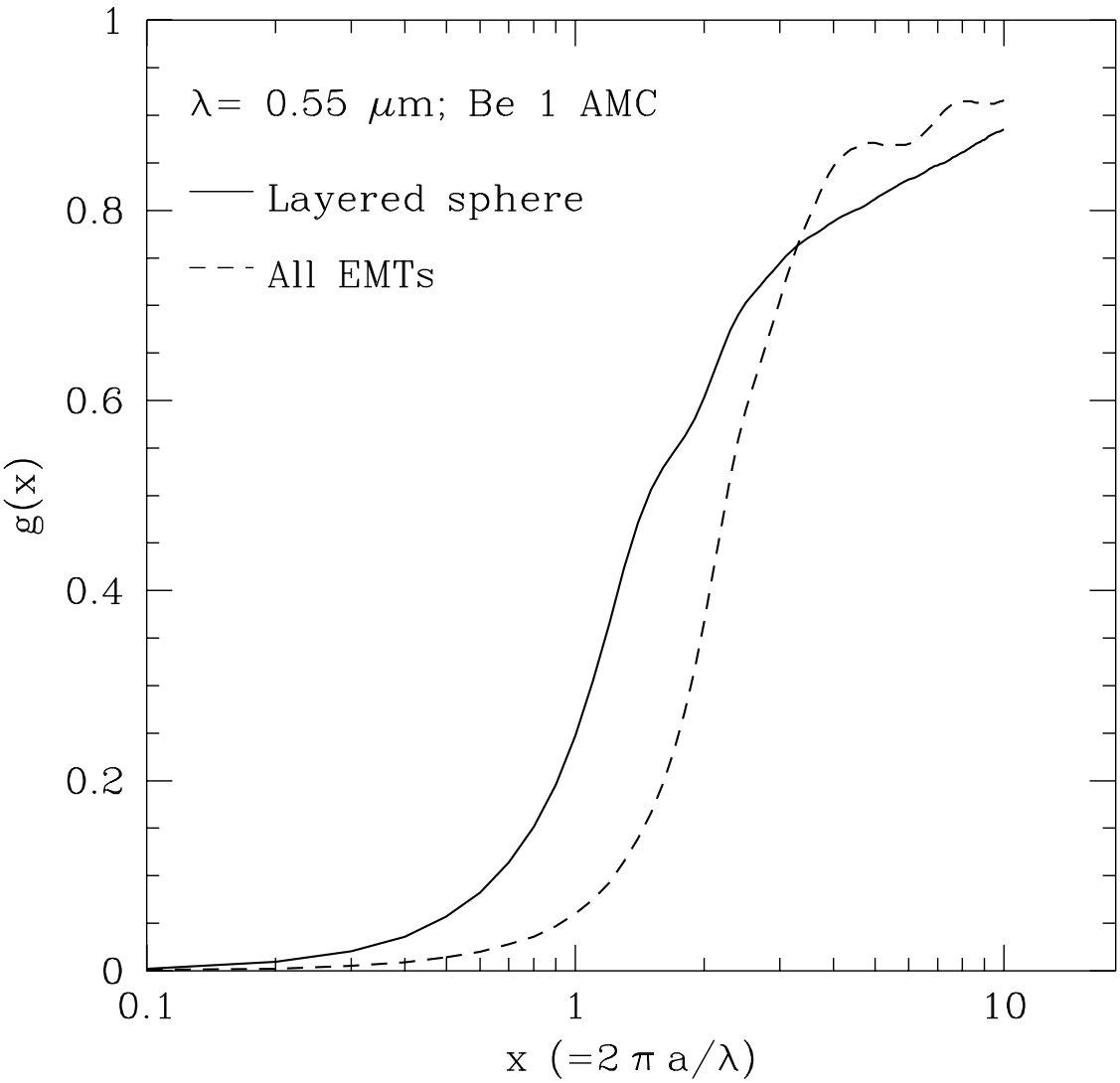

Fig. 6.— The phase parameter $g(x) \equiv \langle \cos(\Theta) \rangle$ for Be 1 AMC, along with 33% vacuum and 33% silicates. The solid line is the layered sphere; various EMTs are identified in the label plotted separately but are indistinguishable. We see that the prediction by the EMTs is poor beyond $x \sim 0.7$, especially for Be 1 AMC, which is less refractive than Jena AMC.